JOURNAL OF GEOPHYSICAL RESEARCH, VOL. 112, F02001, doi:10.1029/2006JF000505, 2007

A technique for the morphological characterization of submarine landscapes as exemplified by debris flows of the Storegga Slide

Aaron Micallef,[1] Christian Berndt,[1] Douglas G. Masson,[1] and Dorrik A. V. Stow[1]

Received 23 March 2006; revised 13 October 2006; accepted 15 November 2006; published 3 April 2007.

[1] In comparison to subaerial and planetary landscapes, submarine environments are rarely investigated using quantitative geomorphological techniques. Application of traditional geomorphometric techniques is hindered by the spatial variability in bathymetric data resolution and the extensive scale over which changes in topography occur. We propose a novel methodology for the improved quantitative analysis of submarine elevation data by adapting numerical techniques, developed for subaerial analyses, to submarine environments. The method integrates three main morphometric techniques: (1) morphometric attributes and their statistical analyses, (2) feature-based quantitative representation, and (3) automated topographic classification. These techniques allow useful morphological information to be extracted from a digital elevation model. Morphometric attributes and their statistical analyses provide summary information about an area, which can be used to calibrate computer-generated geomorphometric maps. In these maps the boundaries of geomorphological features are delineated, and they can thus be used as the basis for geomorphological interpretation. Ridge patterns and their morphological characteristics provide an accurate representation of specific aspects of terrain variability. Moment statistics are used as proxies of surface roughness to differentiate between surface types. Unsupervised classification, carried out using ridge characteristics and moment statistics, reliably segments the surface into units of homogeneous topography. A case study of debris flow lobes within the Storegga Slide shows that the techniques work robustly and that the new methodology integrating all the techniques can significantly enhance submarine geomorphological investigations.

Citation: Micallef, A., C. Berndt, D. G. Masson, and D. A. V. Stow (2007), A technique for the morphological characterization of submarine landscapes as exemplified by debris flows of the Storegga Slide, *J. Geophys. Res.*, *112*, F02001, doi:10.1029/2006JF000505.

1. Introduction

[2] Geomorphometry is the quantitative description of landscapes [*Pike and Dikau*, 1995]. It is based on the assumption that there is a close quantitative relationship between surface processes and topographic characteristics [*Moore et al.*, 1991], and that these characteristics contain geological information that can be extracted by numerical analysis. Since the 1970s geomorphometry has increasingly been based on digital elevation models (DEMs). DEM analyses generally involve the process of taking derivatives of altitude to compute morphometric attributes, and the summarization of these attributes using moment statistics [*Evans*, 1998]. A more thorough investigation is achieved by using spatial derivatives of these initial attributes (e.g., topographic wetness [*Moore and Neiber*, 1989]). An overview of the history and state of the art in geomorphometry is given by *Pike* [2000]. Compared to traditional geomorphological methods, techniques used in general geomorphometry have the benefits of avoiding problems of subjective interpretation and of landform definition prior to analysis. The present challenge in geomorphometry is to delineate landforms from a continuous grid of terrain attributes. This has been dealt with by employing a variety of techniques, among which feature extraction and automated pattern recognition algorithms [e.g., *Chang et al.*, 1998; *Chorowicz et al.*, 1989]. On the whole, however, geomorphometry has remained a nonsystematic set of techniques, and no standardized methodology for the quantitative study of landscapes and the extraction of landforms is available.

[3] Geomorphometry has been applied successfully in a variety of subaerial settings, e.g., fault morphology [*Florinsky*, 1996], drainage basins [*Gardner et al.*, 1990], and deep-seated landsliding [*Roering et al.*, 2005]. Today the discipline is stimulated by the need to explain inaccessible or enigmatic landscapes. Whereas geomorphometric techniques have become a standard tool in the investigation of planetary landscapes [e.g., *Aharonson et al.*, 2001], their application to submarine environments has been more infrequent. Some examples of the latter include the use of spectral models to classify ridge-crest terrains [*Fox*, 1996] and the automated extraction of submarine drainage systems [*Pratson and Ryan*, 1996]. In general, the geological interpretation of submarine landscapes tends to be relatively

[1]National Oceanography Centre, Southampton, UK.

0148-0227/07/2006JF000505$09.00

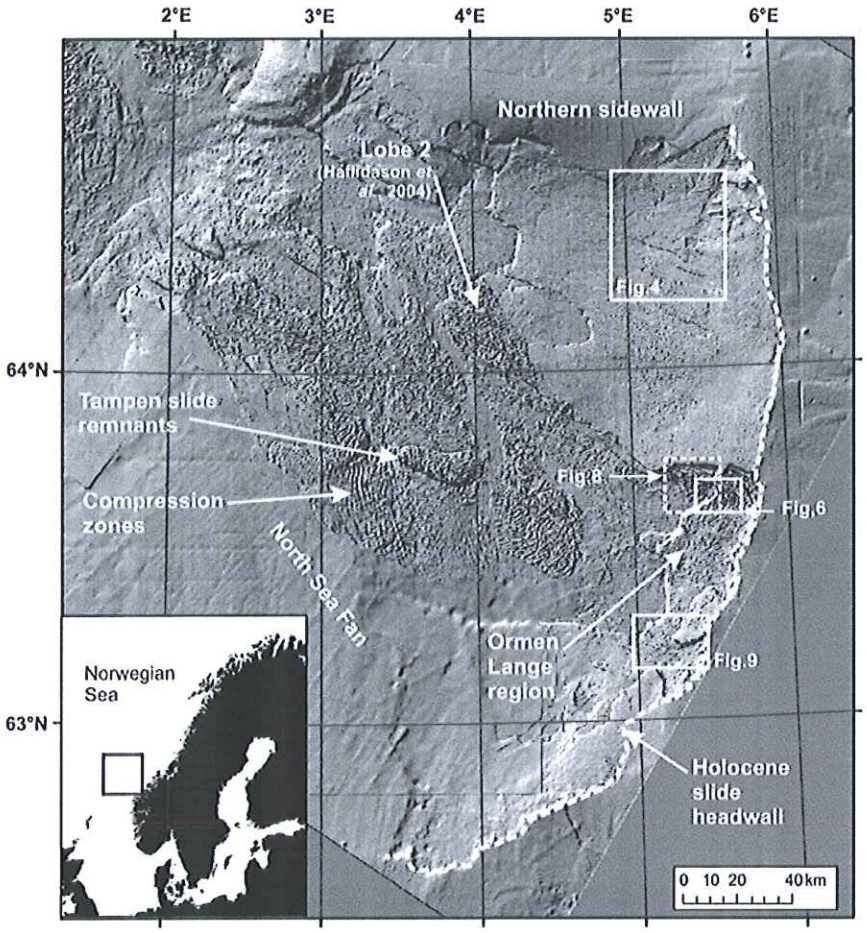

Figure 1. Shaded relief map of the study area and the major topographical features. Boxes indicate the location of Figures 4, 6, 8, and 9.

more subjective, with shaded relief maps being one of the standard tools of bathymetric data representation. Submarine landscapes and bathymetric data have a number of characteristics that makes the application of traditional geomorphometric techniques problematic. First, in comparison to terrestrial landscapes, submarine topographies are generally smoother and changes in elevation occur over more extensive areas [*Shepard*, 1963]. The features of interest are also larger and extend over considerable depth ranges [*Hühnerbach and Masson*, 2004; *Masson et al.*, 2006]. This means that the range of morphometric attributes and their statistics, over which changes in topography can be observed, are in general much narrower than for subaerial landscapes. Capturing submarine terrain variability using traditional geomorphometric techniques is therefore more difficult. Secondly, whereas there exists the possibility of ground-truthing subaerial DEMs and satellite images, this is very hard to achieve in submarine environments. As a result, geomorphometric techniques for the study of submarine landscapes need to be very robust, combining results from a variety of methods to ensure that the outcome is a genuine representation of the topographic variability. Thirdly, since submarine DEMs cover more extensive areas than subaerial DEMs, they are bound to include data sets of different resolutions. The resolution of the same data set is also bound to change with depth [*De Moustier and Matsumoto*, 1993]. The outcomes of geomorphometric techniques depend very much on data resolution [*Evans*, 1975]. Thus integrating results from different techniques should help overcome the sensitivity of the individual techniques to different resolutions.

[4] In this paper we adapt a number of geomorphometric techniques to the submarine environment and propose a methodology for the study of bathymetric data sets. We apply these techniques to a high-resolution bathymetry data set from the Storegga Slide (Figure 1), the largest documented submarine landslide on glacially influenced margins [*Bugge et al.*, 1987; *Canals et al.*, 2004]. Bathymetry data sets contain a wealth of information that is generally not fully exploited by the marine geologist. The very high resolution of our data set, combined with the diversity of topographic features encompassed, makes the Storegga Slide an ideal site for the development of submarine geomorphometric techniques.

[5] The objectives of this study are (1) to adapt established geomorphometric techniques and develop a methodology for the improved quantitative analysis of submarine elevation data and (2) to test the applicability of this

Table 1. Formulae Used to Derive the Morphometric Attributes

Attribute	Formula[a]
Slope gradient	$\arctan(p^2 + q^2)^{1/2}$
Slope aspect	$-90[1 - \text{sign}(q)][1 - \lvert\text{sign}(p)\rvert] + 180[1 + \text{sign}(p) - 180\text{sign}(p)\arccos[-q/(p^2 + q^2)^{1/2}]/\pi$
Profile curvature	$-(p^2r + 2pqs + q^2t)/[(p^2 + q^2)(1 + p^2 + q^2)^{3/2}]$
Plan curvature	$-(q^2r - 2pqs + p^2t)/(p^2 + q^2)^{3/2}$

[a]Where $p = \frac{\partial z}{\partial x}$, $q = \frac{\partial z}{\partial y}$, $r = \frac{\partial^2 z}{\partial x^2}$, $s = \frac{\partial^2 z}{\partial x \partial y}$, and $t = \frac{\partial^2 z}{\partial y^2}$.

methodology by applying it to the morphological interpretation of debris flow deposits.

2. Methodology and Observations

2.1. Data Set Information

[6] The Storegga Slide lies 70–150 km off the western coast of Norway, in the Norwegian Sea (Figure 1), and covers an area of ~95,000 km^2, including 27,000 km^2 of slide scar [*Bryn et al.*, 2003; *Canals et al.*, 2004]. The most recent studies have shown that the Holocene Storegga slide was a multiphase retrogressive event with an estimated volume of 2400–3200 km^3 [*Canals et al.*, 2004; *Haflidason et al.*, 2005]. The slide scar consists of a vast bathymetric depression that includes a variety of mass movement forms, ranging from lateral spreads to turbidity currents.

[7] Our investigation of the Storegga Slide is based on high-quality bathymetry data provided by Norsk Hydro AS. These data comprise the Storegga Slide seafloor from the slide headwalls at the continental shelf edge down to a water depth of 2700 m. The horizontal resolution varies from 5 m grids in the Ormen Lange area, to 9 km grids in the southern part of the study area (ETOPO5 data), although most of the area is covered by data of 25 m resolution or better. The vertical resolution varies from ±10 cm to 2 m at depths of up to 800 m, to ±10 m at 2000 m depths or more (E. Sletten-Andersen, personal communication, 2005).

[8] For this study, we selected an area that includes the main scar of the Storegga Slide, extracting 53 million elevation data points that are represented in a DEM with a cell size of 25 m × 25 m. This was done by interpolation in areas of coarser resolution and aggregation using means in higher-resolution areas. The selected resolution of the DEM was found adequate for subaerial slope analysis by *Nogami* [1995]. All techniques are tested in areas where the original data had a resolution of 25 m or better.

2.2. Morphometric Attributes and Statistics

[9] The process of calculating derivatives to obtain morphometric attributes, and of summarizing their frequency distributions by taking moment statistics, has been at the basis of altitudinal data analyses since the 1970s [*Evans*, 1980]. The importance of altitude and its primary and secondary derivatives (slope and curvature) to geomorphological studies was recognized by *Curtis et al.* [1965] and *Anhert* [1970] in pedological and slope morphology studies, respectively. The technique was incorporated into geomorphometric systems by *Evans* [1972]. Since then, frequency distribution based characterizations of a range of different settings have been carried out (e.g., slope instability [*Carrara et al.*, 1977] and hillslope mapping [*Evans*, 1979]).

[10] We started our investigation of the Storegga Slide by computing the following digital morphometric maps of the study area using the Geographic Information System (GIS) ArcGIS: (1) shaded relief map (using 3X exaggeration and NW illumination), (2) slope gradient map (in degrees), (3) slope aspect map (in degrees), (4) profile curvature map (in degrees m^{-1}), and (5) plan curvature map (in degrees m^{-1}). The attributes were extracted for 3 × 3 cell neighborhoods using the equations in Table 1. The frequency distributions of the morphometric attribute data are presented in Figure 2. The frequency distribution of slope gradient data is unimodal and highly positively skewed (Figure 2a). This results from the fact that the Storegga Slide is located in a gently dipping depositional environment on a continental slope. The cumulative frequency distribution for the slope gradient shows that, for 90% of the area, the slope gradient is <4°, while almost 57% of the terrain has a slope gradient <1°. The point of inflection in this curve is positioned at a slope gradient of 5° (Figure 2a). This separates lower-relief and gentler topography from more prominent geomorphological features such as headwalls and blocks in the Ormen Lange region, Lobe 2, Tampen slide remnants, compression zones, and downslope headwalls. This slope angle is considered an important threshold in the slope gradient distribution. When analyzed on a circular scale, the mean and standard deviation of slope aspect were determined to be 290.36° and 70.04°, respectively (Figure 2b). The slope aspect frequency distribution maxima occur at the NW (315°), W (270°) and SW (225°) directions, with N (0°) having the highest frequency. The graph is characterized by peaks occurring at 45° intervals. The frequency distributions for the curvatures are unimodal and almost symmetrical, and as such do not provide much additional information.

[11] Bivariate analysis extracts relationships between pairs of morphometric attributes across a DEM. As an example, slope gradient is plotted against slope aspect in Figure 2c. Because of the very large number of data points in the study area, data were resampled at 2%, resulting in ~1 million values for each morphometric attribute. The resulting plot is dominated by three peaks. It shows that slopes tend to be steeper than average if they face NNE, SW or NW. When the peaks were displayed on a combined slope gradient-slope aspect map and a shaded relief map, they were found to correspond to the major headwalls in the Storegga Slide. The highest peak displayed is for the NW direction and corresponds to the main slide headwall.

2.3. Feature-Based Quantitative Representation

[12] Feature-based quantitative representation describes the morphology of an area through the geometric attributes of individual landforms. Individual or groups of algorithms are applied to classify relief or morphometric attributes into

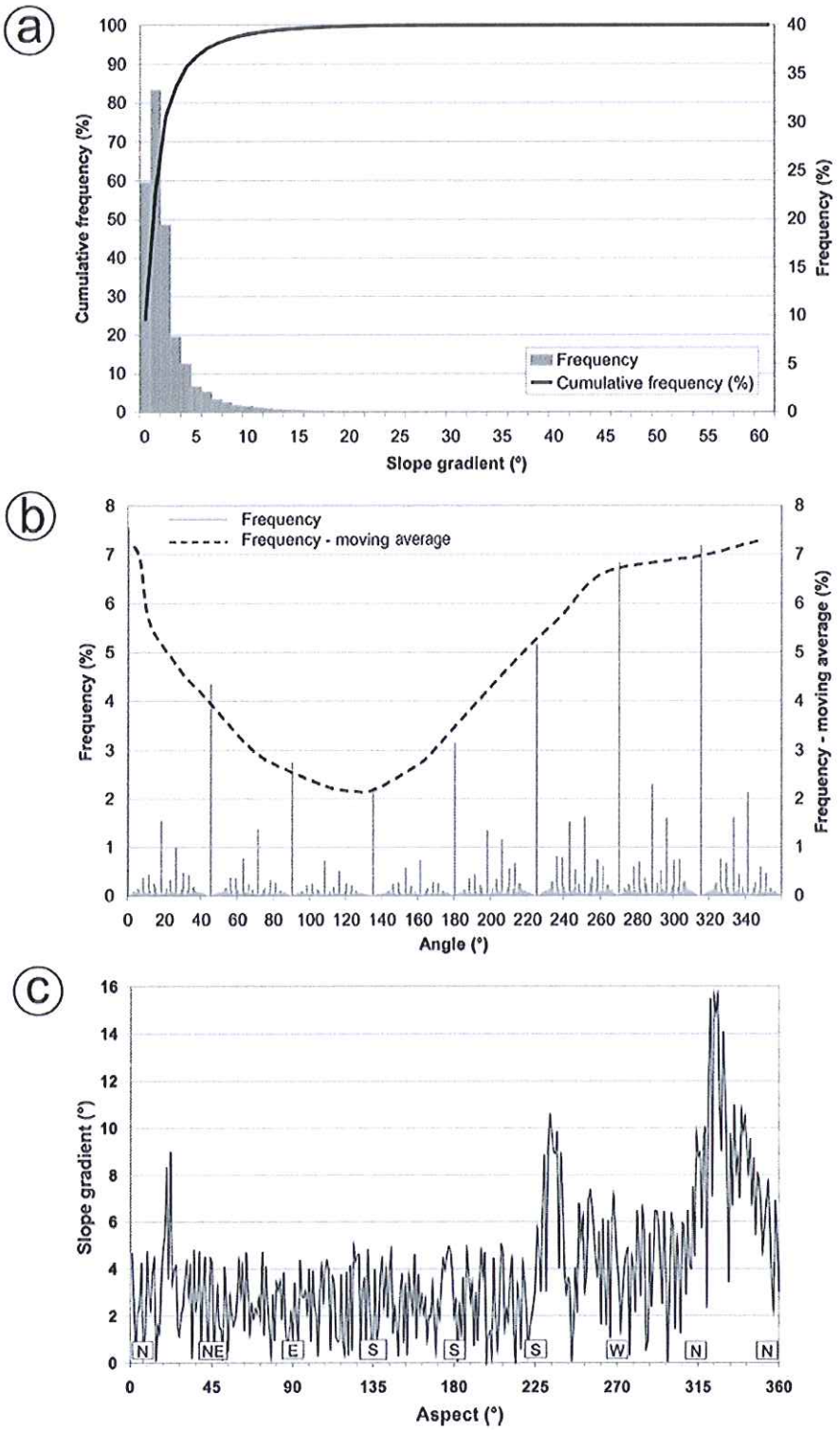

Figure 2. Frequency and cumulative frequency distribution for (a) slope gradient and (b) slope aspect, with moving average. (c) Plot of slope gradient against slope aspect for a 2% sample of the bathymetric data from the Storegga Slide.

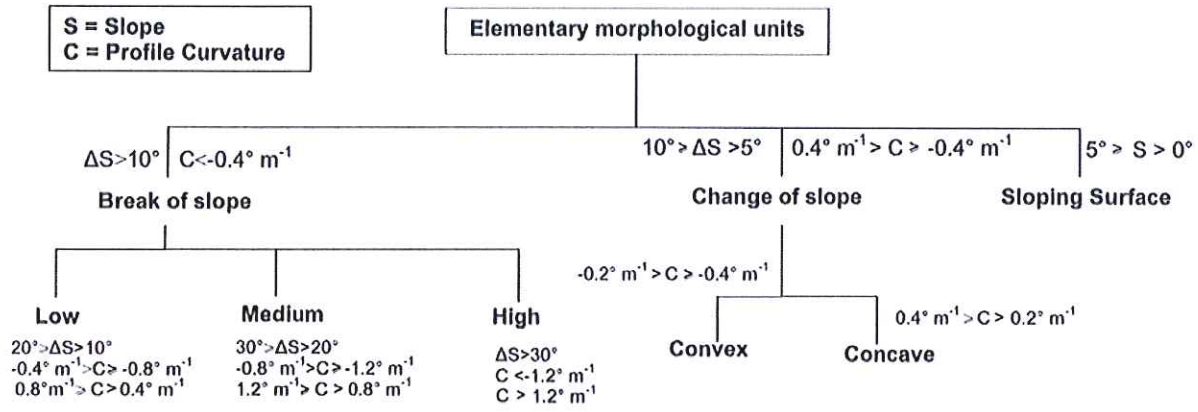

Figure 3. Dendrogram of the elementary morphological units based on the survey of 10 testing areas within the Storegga Slide.

a number of classes of simple forms. Examples of this technique include the extraction of fluvial networks [*Chorowicz et al.*, 1992] and the identification of linear and circular features from satellite imagery [*Raghavan et al.*, 1995].

2.3.1. Geomorphometric Mapping

[13] Initially, we delineate the boundaries of finite geomorphometric objects from the continuous grid of morphometric attributes. We do this by generating a geomorphometric map, which is a parametric representation of the general morphology of a landscape. The process entails the identification of morphometric attributes, computational slicing of the domain of each attribute into intervals, and mapping of these intervals. This approach of topographic parameterization, particularly the use of breaks of slope to identify the boundaries of slope units, is inspired by techniques used in subaerial geomorphological mapping [e.g., *Gardiner and Dackombe*, 1983; *Parsons*, 1988]. A virtual field study was carried out, using a 3-D visualization of bathymetry, to identify the elementary morphological units of the landscape. The four fundamental features recognized were the following.

[14] 1. Break of slope is a change in slope gradient between adjacent cells that is higher than 10°. This feature was divided into three groups: low (10°–20°), medium (20°–30°), and high (>30°).

[15] 2. Change of slope is a change in slope that is >5° and <10°. Changes of slope can be either convex or concave.

[16] 3. Sloping surface is an area, larger than 1 km^2, with a constant slope aspect and gradient, the latter being <5°.

[17] 4. Blocks and ridges are features of positive relief that occur either in isolation or in a repetitive pattern.

[18] A dendrogram (Figure 3), which attributes a range of morphometric attribute values to the first three features, was constructed. The extraction of blocks and ridges is described in detail in section 2.3.2. The choice of the thresholds of the ranges for each morphometric attribute was based on observations of the morphometric attribute maps, on their frequency distributions and moment statistics. As an example, the lower limit for changes of slope is based on the turning point identified in the cumulative frequency curve of slope gradient occurring at 5° (Figures 2a and 3). We simplified the technique by restricting the use of attributes as discriminating variables to profile curvature, slope gradient, slope aspect and elevation differences, which have previously been shown to be effective in describing subaerial landforms [e.g., *Giles*, 1998; *Graff and Usery*, 1993]. We then extracted each feature based on the dendrogram. To extract the breaks and changes of slope, the profile curvature raster image was reclassified into the five classes of profile curvature specified in the dendrogram (Figure 3). In this way, a range of profile curvature values was flagged to a class, which made it possible to contour each class separately. The height of the break of slope was calculated for 200 points using trigonometry. The sloping surfaces were extracted by first generating a slope aspect map of the study area with a cell size of 1 km × 1 km. Then a contour map of slope gradient for the range 0°–5° was produced at 0.5° intervals, displaying regions of constant slope. The two maps were combined, and slope arrows were manually drawn in areas of constant aspect bounded by a slope contour. The slope direction was read from the aspect map while the slope gradient was derived from the slope contour map.

[19] Figure 4 shows a geomorphometric map displaying the above fundamental morphometric features for a part of the Storegga Slide. Interpretation of the geomorphometric map is best carried out using all geological knowledge available for the area. The extracted lineaments mainly correspond to boundaries of geomorphological features. For instance, the breaks of slope shaped in a Z form in the south central part of the map correspond to the flanks of a debris flow (north) and a slab slide (south). The height of these sidewalls ranges between 32 m and 39 m. In the northeastern part of the map are located two elliptical features and an extensive void area. These represent two spurs located upslope of the exposed failure plane of Lobe 1 [*Haflidason et al.*, 2004]. In order to verify whether the extracted lineaments do correspond to actual morpho-

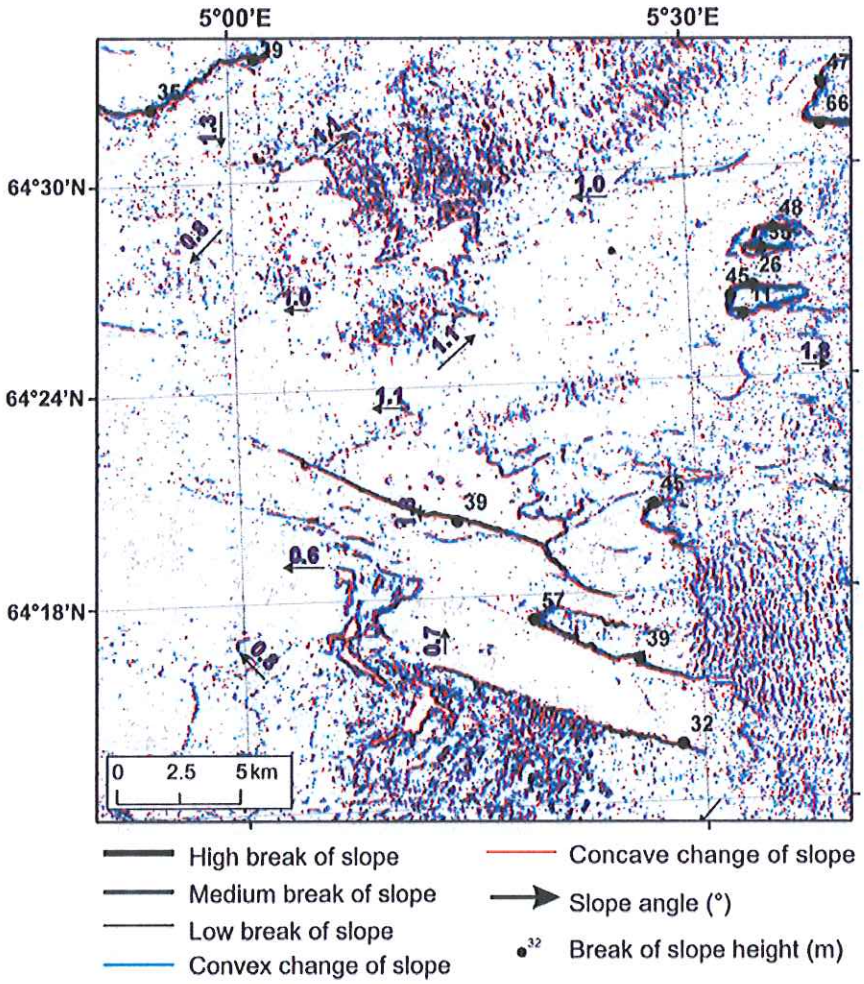

Figure 4. Part of the geomorphometric map south of the northern sidewall, with breaks of slope, changes of slope, sloping surfaces, and breaks of slope heights.

logical features, the geomorphometric map from a different part of the Storegga Slide was draped over a 3-D visualization of the bathymetry, as shown in Figure 5. A low break of slope is located at the top of the 150 m high headwall where the terrain suddenly becomes steeper, whereas a concave change of slope follows the foot of the scarp where the terrain is gentler. Additionally, a convex change of slope exists in the central part of the headwall slope.

2.3.2. Ridge Characterization

[20] The Storegga Slide scar is characterized by a topography that is quite different to what is generally observed in subaerial landscapes. Apart from the headwalls and scars, the various sediment mobilization and deposition processes within Storegga have resulted in a surface that consists of an extensive pattern of ridges and blocks. This pattern yields additional geomorphological information to that garnered from the breaks and changes of slope, and it was fundamental to *Haflidason et al.* [2004] to extract slide lobes in the Storegga Slide. The pattern in the study area ranges from the linear and repetitive to blocky and chaotic. For simplicity, we refer to this pattern as a ridge pattern from this point forward. Although the ridge pattern is occasionally picked out by the geomorphometric mapping technique explained earlier, here we propose a method for the systematic extraction of the pattern and associated morphological characteristics.

[21] Ridges in the Storegga Slide were characterized using a suite of GIS tools. The ridge extraction approach involves implementing a runoff simulation technique to the Storegga Slide by considering the DEM as a dry impervious subaerial landscape. If a hypothetical precipitation event was to take place, water runoff would be expected to flow down the ridges' sides, accumulating in the troughs and leaving the crests dry. Thus a standard GIS hydrology tool known as flow direction routine can be applied to the elevation data set to generate a raster file representing the theoretical flow direction of water in each raster cell. This file was then used in another GIS tool, known as flow accumulation routine, which created a raster file of accumulated flow to each cell by summing the weight of all cells that flow into each cell downslope. Since ridge crests would constitute the driest part of the landscape, they have zero

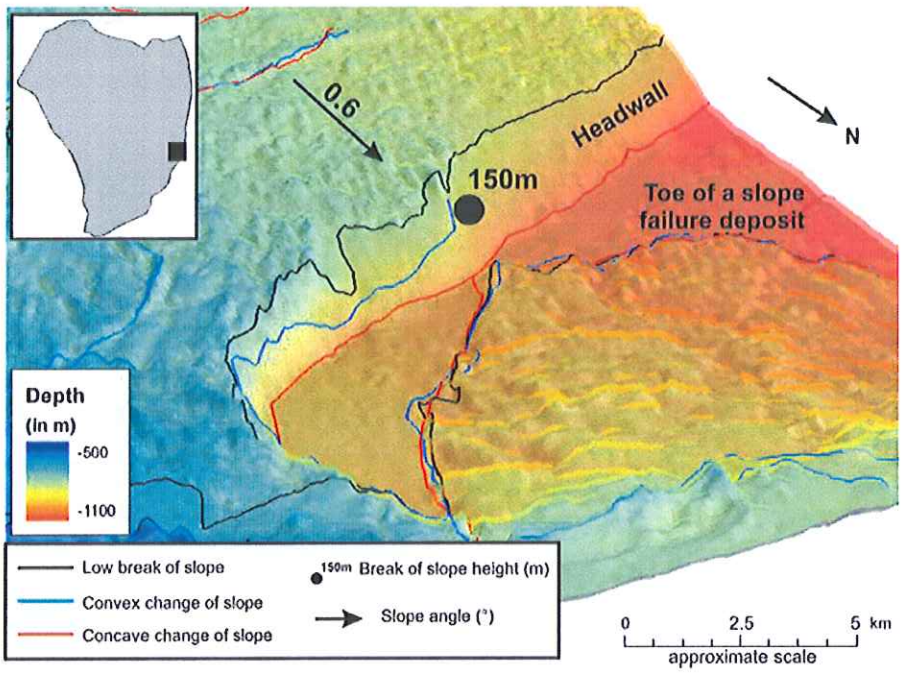

Figure 5. Geomorphometric map of a part of the Storegga Slide draped over a 3-D visualization of the landscape, showing that the numerical methods are able to extract geomorphometric elements reliably. Note the convex change of slope within the slide headwall, which could have been easily overlooked in a manual interpretation.

flow accumulation. Thus we extracted these cells. In this way, all the ridges in the study area were automatically vectorized and could be used for further ridge analysis. The resulting pattern is very detailed, counting 1.2 million lines, and is best observed on large maps. A part of the extracted ridge pattern is displayed in Figures 6a–6d. A transect across a part of this ridge pattern displays the location of the extracted ridges as black dots above the corresponding bathymetric profile (Figure 6e). The ridge map was also draped over a 3-D visualization of the bathymetry to validate that the extracted ridge pattern corresponds to the ridge crests.

[22] Using the digital ridge map it was possible to extract five ridge characteristics: direction, trough depth, density, spacing and length. To obtain ridge direction, we divided the ridge pattern vector file into a 500 m × 500 m grid, and a linear directional mean tool was applied to each grid cell. This tool calculates the mean orientation of lines inside each cell. This resulted in 0.25 km^2 cells representing the orientation of lines in degrees. Figure 6a indicates how the direction of the ridge pattern in two adjacent cells can be different, with the ridges in the southern box having a more northerly direction than the ridges in the northern box. The map differentiates the two patterns by attributing different values for the mean ridge direction.

[23] Trough depth can be extracted using the flow accumulation raster image generated earlier. The elevations for the cells with zero flow accumulation values were extracted, converted into a point vector file, and interpolated to generate a raster surface that links the tops of all the crests. The interpolated surface was then subtracted from the original elevation raster image to produce a map of trough depths, which corresponds to the inverse of ridge heights. A comparison between the bathymetric profile and the trough depth curve for a 4 km transect clearly shows that the trough depth peaks coincide with the troughs in between ridges, so that the deeper the ridges, the higher the peaks of the trough depth curve (Figure 6e).

[24] Ridge density, i.e., the total number of ridge lines per unit area, was calculated by applying the line density function to 500 m × 500 m cells to the ridge pattern map (Figure 6b). Ridges in the southern box on Figure 6c are more frequent than those in northern box. The ridge density map portrays this by assigning values of 8.4–15.9 km^{-2} to the southern box, compared to values 1.7–7.3 km^{-2} for the northern box.

[25] Ridge spacing was determined by converting the ridge pattern to a raster file. The distance of each cell from the closest ridge cell was measured using the Euclidean distance tool in GIS. The peak values of the generated distance raster file, which correspond to the highest distance of single cells from two adjacent ridges, were extracted in the same way as the ridge pattern was extracted from the elevation data set earlier. Once the peak values were available, they were multiplied by 2 to represent the spacing between two ridges. Figure 6c shows how the technique differentiates between the widely spaced ridges in the northern box and the closely spaced ridges in the southern box.

[26] Finally, the length of each ridge was measured using the x and y coordinates of the ridge line vertices, and a mean value was taken for a grid cell with dimensions

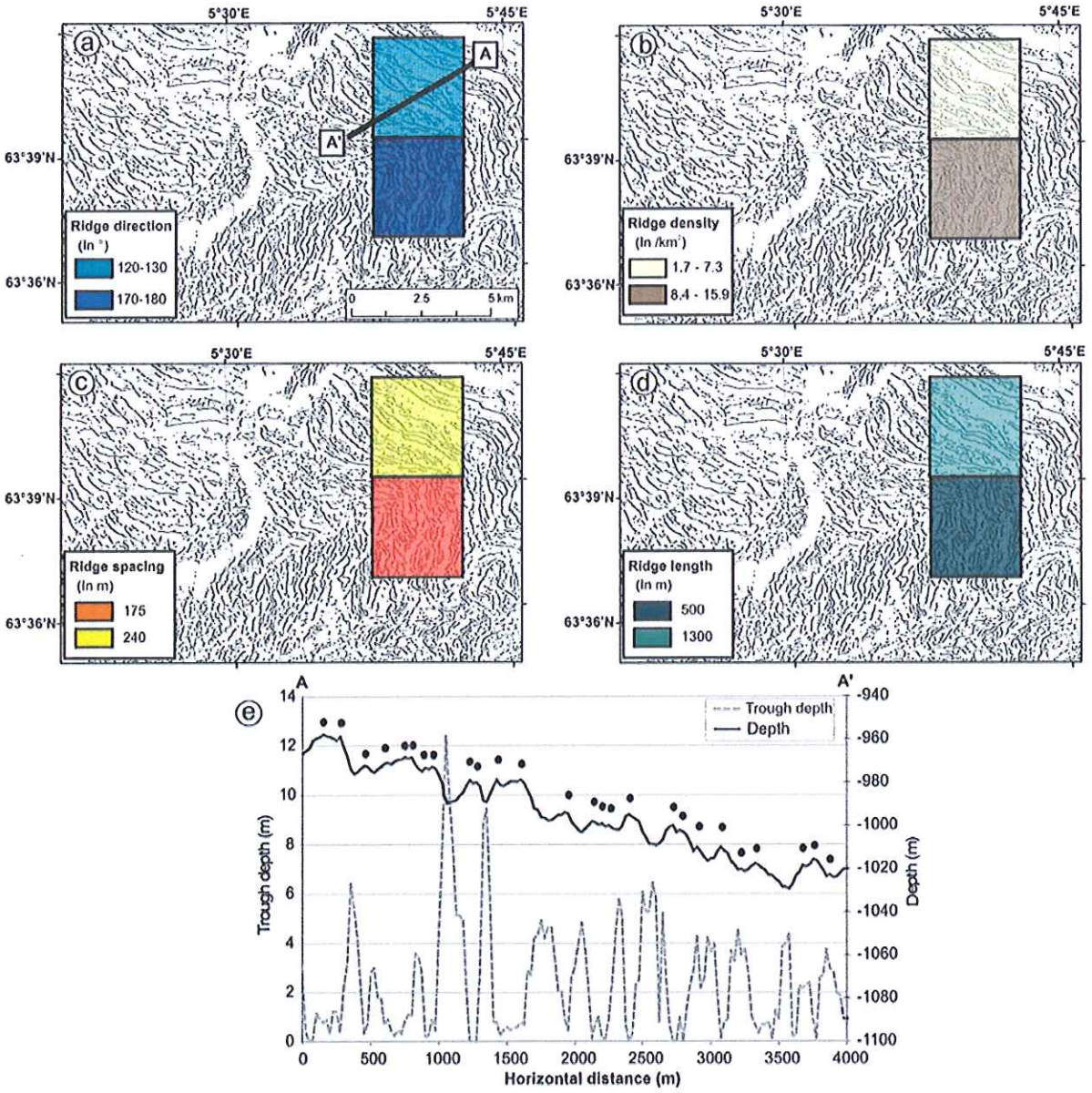

Figure 6. Ridge pattern maps for the northern Ormen Lange region, with two squares from (a) the ridge direction map, (b) the ridge density map, (c) ridge spacing map, and (d) ridge length map. The squares combine the ridge characteristic values over an area of 2.5 km × 2.5 km. (e) Comparison of the bathymetric profile for a 4 km transect, shown in Figure 6a, with the trough depth curve. The black dots indicate the position of the identified ridges in the ridge pattern map.

500 m × 500 m. In Figure 6d, the shorter ridges in the southern box are assigned a mean ridge length of 500 m, whereas the calculated mean length for ridges in the northern box is 1300 m.

2.4. Automated Topographic Classification

[27] So far we have concentrated on the identification of geomorphometric elements and boundaries as linear features. Also important for a thorough morphological assessment of a landscape is its segmentation into homogeneous relief units enclosing regions with uniform landform distribution. The assumption for using this technique is that similar geological and geomorphological processes operate within regions sharing similar topographies [*Etzelmüller and Sulebak*, 2000]. We classify the Storegga Slide surface using two approaches.

2.4.1. Moment Statistics

[28] The first type of classification is based on the concept of surface roughness. Surface roughness has been defined in different ways in the past [*Evans*, 1990] and it lacks a definite measurement scale. In this paper we define surface roughness as the deviation of the terrain surface

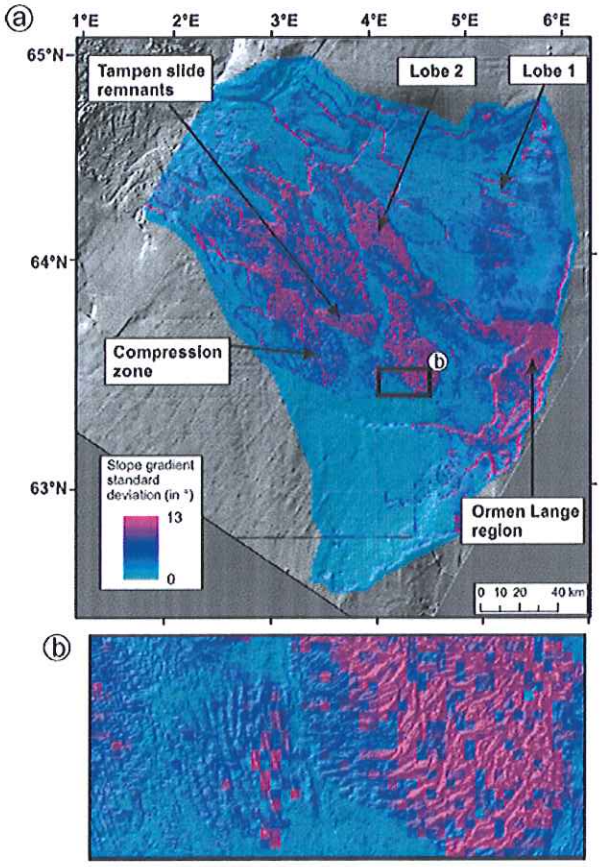

Figure 7. (a) Slope gradient standard deviation map of the Storegga Slide and the main topographic features. (b) Enlargement of the area enclosed by the black box, showing a progressive increase in surface roughness eastward.

from a perfectly smooth terrain due to the presence of irregular features. The greater the height between the apex of the feature and the surrounding terrain, and the more frequent the features are, the higher the surface roughness. Therefore the presence of features such as ridges, headwalls and blocky deposits increases the surface roughness of the terrain. *Evans* [1990] suggested that the following moment statistics of morphometric attributes can be used in measuring components of surface roughness: mean and standard deviation of slope gradient, and standard deviation of elevation, profile and plan curvature. Here we calculated these five moment statistics for grid cells 500 m × 500 m in area.

[29] Figure 7a shows the spatial variation of the standard deviation of slope gradient. All the moment statistics are highly correlated (Table 2). Thus only the standard deviation of slope gradient is considered in detail. The highest values for the slope gradient standard deviation are found in the headwalls, scarps, blocky deposits, Tampen slide remnants, Ormen Lange region and Lobe 2 deposits. For example, the headwalls and lateral spreads in the northern part of the Ormen Lange region are characterized by high values of slope gradient standard deviation, whereas lower values are recorded in the failure plane of Lobe 1 located just north of this region. A more detailed inspection of the slope gradient standard deviation map draped on the shaded relief map (Figure 7b) confirms that a progressive reduction in slope gradient standard deviation westward is equivalent to a lower surface roughness, which is distinguished by fewer and shallower ridges.

2.4.2. ISODATA

[30] The second method involves the description of multivariate data in terms of clusters of data points that possess strong internal similarities [*Duda and Hart*, 1973]. One of the most widely used unsupervised clustering algorithms is Iterative Self-Organizing Data Analysis Technique (ISODATA). This technique defines natural groupings of multivariate data in attribute space [*Adediran et al.*, 2004] and is a commonly used algorithm in satellite image classification and civil engineering [*Hall and Khanna*, 1977]. The ISODATA method uses the Euclidean distance between each pair of data points in a k-dimensional attribute space to form clusters. The technique is based upon estimating some reasonable assignment of cells to candidate clusters, and then moving them from one cluster to another so that the sum of the squared errors of the preceding session is reduced. The output of the classification is a digital thematic map where each cluster is represented by a different class. More detail on the technique is given by *Richards* [1986]. There are several examples of ISODATA being applied to subaerial settings by using morphometric attributes as the input layers. In general, the technique has proved successful at improving the classification of landscapes and extracting morpho-units. *Adediran et al.* [2004] use slope gradient and slope aspect in the classification of a study area in north central Crete, whereas *Sulebak et al.* [1997] apply the technique in Norway using slope gradient and curvature. *Irvin et al.* [1997] use elevation, slope gradient, profile and tangent curvature, topographic wetness index and incident solar radiation as layers for the classification of a valley in Wisconsin, United States, whereas

Table 2. Correlation of the Five Moment Statistics Used to Represent Surface Roughness

	Mean of Slope Gradient	Standard Deviation of Slope Gradient	Standard Deviation of Elevation	Standard Deviation of Profile Curvature	Standard Deviation of Plan Curvature
Mean of slope gradient	-	0.90	0.82	0.89	0.81
Standard deviation of slope gradient	0.90	-	0.82	0.90	0.91
Standard deviation of elevation	0.82	0.82	-	0.79	0.83
Standard deviation of profile curvature	0.89	0.90	0.79	-	0.85
Standard deviation of plan curvature	0.81	0.91	0.83	0.85	-

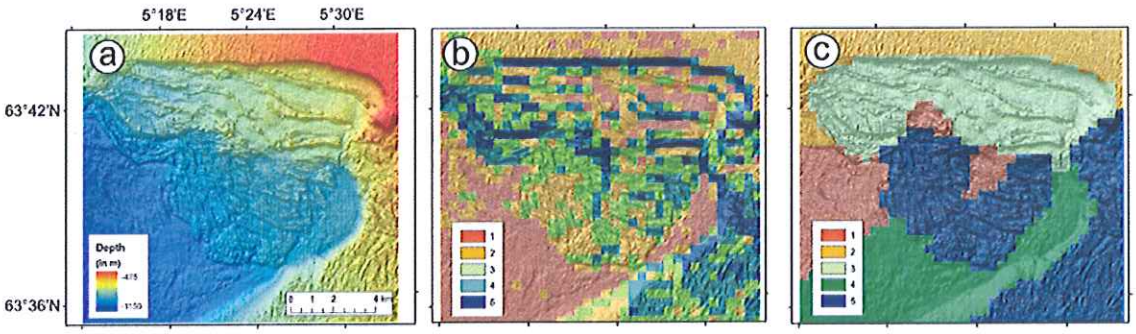

Figure 8. (a) Bathymetry of a landslide located north of the Ormen Lange region. (b) ISODATA thematic map produced with slope gradient, profile, and plan curvature as input layers. (c) ISODATA thematic map produced with the five ridge characteristics and slope gradient standard deviation as the input layers. In both Figures 8b and 8c the image has been draped over a shaded relief map of the area.

Medler and Yool [1998] test the technique using elevation, slope gradient and slope aspect.

[31] This method of classification was applied using two sets of layers. In the first instance, ISODATA was applied to the Storegga Slide using the slope gradient, profile curvature and plan curvature morphometric attribute maps as layers for the classification. In the second set, the input layers used were the standard deviation of slope gradient and the five ridge characteristics maps. For both sets the data were aggregated into 500 m × 500 m cells. In both cases, the number of classes was limited to five, because tests carried out using a higher number of classes did not generate significantly different results.

[32] The thematic maps generated by using ISODATA are shown in Figures 8b and 8c. These were evaluated by comparing them with a shaded relief map (Figure 8a) and a 3-D visualization. The thematic map produced by the first set of layers (Figure 8b) is dominated by scattered cells rather than a continuous coverage by cells from the same class, although a pattern can be distinguished. Class 1 covers the smoother part of the seabed, whereas class 2 is representative of the repetitive pattern of shallow and short ridges located upslope of the headwall. Class 4 partly covers the deeper ridges in the southeastern part of the image. Otherwise, the pattern is chaotic, even if a low-pass filter is applied to it. Figure 8c is the thematic map produced by the second set of layers. It is immediately apparent that the coverage by each class is more continuous. The deep and widely spaced ridges of class 3 are differentiated from the more closely spaced parallel pattern of class 2. Class 5 corresponds to the more disorganized pattern of deeper ridges, whereas the smooth terrain is represented by class 4. On the whole, the classification of the terrain is much improved compared to that in Figure 8b.

3. Discussion

3.1. Morphometric Attributes and Statistics

[33] Frequency distributions of morphometric attributes and their moment statistics provide morphological information and reveal patterns in a complex landscape. Bivariate analysis, in particular, can be used to examine the relationship between different morphometric attributes of single points in a DEM. This provides morphological information about particular features of the landscape, such as headwalls (Figure 2c), and makes them simpler to extract. The information is derived in quantitative form, allowing comparison between different landscapes. The technique also proves useful in providing values for thresholds to be used in geomorphometric mapping. However, it seems that only a limited amount of information may be obtained by applying these geomorphometric techniques to submarine landscapes. The slope gradient frequency distribution is very positively skewed and the majority of the data points are concentrated within a small range. This occurs because changes in elevations in submarine landscapes occur on a much larger scale compared to subaerial landscapes [*Shepard*, 1963]. In addition, the frequency distribution of slope aspect data points is characterized by an overrepresentation of the 45° intervals. This occurs because aspect algorithms do not work well in low-relief regions [*Guth*, 2003]. These characteristics reduce the potential of using slope gradient, slope aspect and their derivatives to discriminate between different submarine landscapes. Overall, the frequency distributions and moment statistics of morphometric attributes should only be used for generating summary information about the morphology of a landscape.

3.2. Geomorphometric Mapping

[34] The geomorphometric map in Figure 4 displays a complex landscape decomposed into its most elementary morphological units. The units are extracted automatically as lineaments that are complemented by topographic information, such as changes in slope gradient and break of slope heights. Draping the geomorphometric map on a shaded relief map and 3-D visualization of the terrain shows that the extracted elements coincide precisely with the features they are supposed to represent (Figure 5). Using this technique on an example site, we were able to identify a convex change of slope in the middle of a steep headwall. This would have been difficult to distinguish if we only based our study on a qualitative interpretation of the site. Geomorphometric mapping is based entirely on the identification and portrayal of changes of form of the slide surface in two dimensions. This excludes the subjective interpretation of the data set and enhances the accuracy of the

morphological investigation. The spatial detail of the digitally generated geomorphometric maps only depends on the resolution of the bathymetric data set rather than the scale at which an observer is investigating the landscape. This ensures that the maximum amount of information available from the DEM is obtained. The only subjective component of this technique is that the user has to define thresholds for the identification of the different features. Because different values for the thresholds can be chosen, this offers versatility in the choice of what morphological units to extract from the bathymetry data set.

[35] The two main drawbacks associated with this technique are that, as in seismic interpretation, correlations between complex landforms may be more easily picked by a human interpreter than by a computer, and that the resolution of the bathymetry data set does have a significant effect on the extraction process. This is evident in the southern part of the Storegga Slide, where data resolution is lowest and where hardly any features were identified. On the whole, computerized geomorphometric mapping is an efficient and versatile technique that produces a simplified representation of landscape in a quick and objective manner.

3.3. Ridge Characterization

[36] The ridge pattern identified by the ridge extraction technique is observed to correspond to the bathymetric ridge crests (Figure 6), confirming the ability of the technique to identify ridge features in the bathymetric data set. The very detailed ridge pattern is in vector format, which permits the application of lineament analysis [e.g., *Casas et al.*, 2000]. The ridge characteristic maps distinguish between the different patterns of ridge directions, heights, densities, spacing and lengths (Figure 6). In this way these maps assist interpretation by extracting additional topographic information and organizing it into manageable grid sizes, as specified by the user. In contrast to the use of moment statistics, the user can control the aspects of ridge morphology on which to base his topographic classification.

[37] The digitally extracted ridge characteristics can also be used for further morphometric analysis; one can plot frequency distributions, calculate their moment statistics, and analyze their spatial pattern. For example, the trough depth map may be used as an accurate representation of surface roughness, as defined in this paper. The mean trough depth would thus correspond to roughness whereas the standard deviation would represent the variation of roughness within an area. Ridge direction, on the other hand, could be used to measure orderliness: The higher the standard deviation of the ridge direction, the more randomly orientated the features are.

3.4. Automated Classification

[38] A qualitative inspection of the map in Figure 7 establishes that the highest values of the moment statistics of morphometric attributes coincide with the most evident irregularities in the terrain such as blocky debris flow deposits, lateral spreading in the Ormen Lange region, compression zones and headwalls. This shows that moment statistics are good proxies for surface roughness. The method is robust and it does not depend strongly on the choice of attribute. On the other hand, the fact that the five moment statistic maps are very similar to each other indicates that, unlike in subaerial landscapes, terrain variability can be described by a few descriptors. This may be practical for classification purposes, but it means that numerous properties of the surface morphology are not being accounted for.

[39] We try to circumvent these problems by combining two types of topographic classification and using as much morphometric information as possible. By introducing moment statistics and ridge characteristics in the ISODATA classification, rather than using the conventional elevation and morphometric attributes, a more accurate and continuous coverage of ridge morphologies is achieved. The surface morphology is well differentiated by the classes, as shown by the different classes representing different ridge lengths, spacings and trough depths in Figure 8c. The main advantage of ISODATA is that it generates summary information about a landscape that is easy to interpret and provides a simplified overview of a complex landscape. The technique is also quick, which allows different combinations of morphometric attributes to be tested. The main disadvantage of ISODATA is that of any unsupervised classification: Prior knowledge of the landforms is essential for the results of the classification to be interpreted to their full potential.

[40] There is an extension of the automated topographic classification, which is not discussed further in this paper. The ISODATA technique also generates a signature file that lists the value limits of the input layers used for each class. These limits can be utilized in a supervised classification of the same input layers over a larger area. If classes can be flagged to particular geomorphological features, it would be possible to extract landforms automatically using this technique.

4. Application of the Techniques for the Identification of Debris Flow Lobes

[41] A part of the Storegga Slide, the Ormen Lange region, was chosen to test the performance of the proposed geomorphometric techniques in the identification of debris flow lobes (Figure 9a). This region is ideal for this study because the original morphology of the debris flow deposits has not been overprinted by subsequently deposited slide material, and the data resolution is highest in this part of the Storegga Slide.

[42] The dominant mass movement types in the southern part of Ormen Lange are debris flows. A debris flow is a rapid, non-Newtonian flow of dense sediment that covers long distances. The main sediment support system within a debris flow is the strength of the matrix [*Mulder and Cochonat*, 1996]. Three distinct morphological units characterize a typical debris flow [*Corominas et al.*, 1996]: a source, a track and an accumulation zone. The source region is generally characterized by a headwall. The track is the section where material is transmitted from the source to the accumulation zone and lacks the surface roughness that distinguishes the accumulation zone. The accumulation zone comprises single or overlapping debris flows deposited at the foot of the track in the form of an expanded lobe with steep margins [*Johnson*, 1984]. The longitudinal profile of the accumulation zone consists of elevated terrain with a convex terminal snout. These are represented as a convex

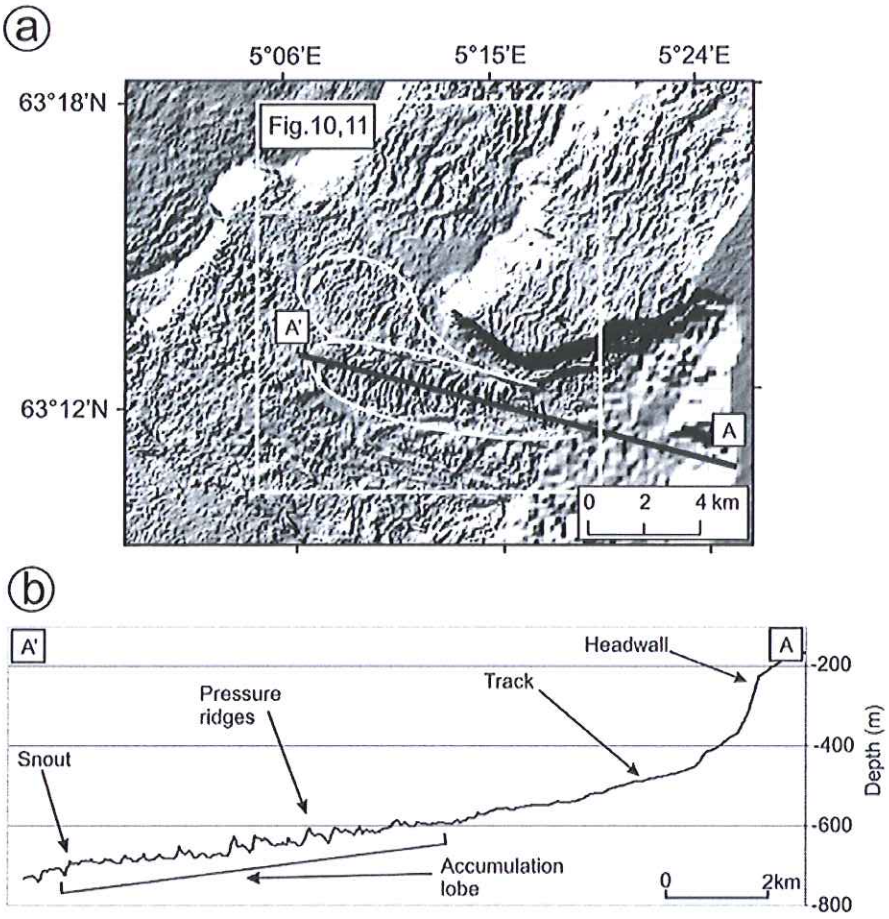

Figure 9. (a) Shaded relief map of the two debris flow lobes identified in the southern part of the Ormen Lange region (the white lines indicate the boundaries of the lobes). (b) Profile of the transect shown in Figure 9a.

change of slope bordered by a concave change of slope. The surface of the accumulation zone may be characterized by rough terrain due to the presence of transverse pressure ridges [*Prior et al.*, 1982] and lateral levee deposits [*Nygård et al.*, 2002]. These features are distinguished by convex crests enclosed by parallel concave changes in slope.

[43] We identified the accumulation zones of two debris flow lobes to test how geomorphometric techniques performed in identifying this type of feature (Figure 9a). When investigated in a 3-D visualization of bathymetry, these two features are seen to exhibit all the characteristics of debris flows: elevated accumulation zone with a rougher texture and a lobate form, and linear levees on the flanks. An east-west transect across the southern lobe shows a typical profile of a debris flow lobe (Figure 9b). From this plot it is observed that the main headwall of the Storegga Slide constitutes the source of the sediment for the debris flow, which has moved across a relatively steep and smooth track, at the end of which it deposited the sediment in accumulation lobes with pressure ridges and a convex snout.

[44] Having identified the debris flow lobes, we tested how the geomorphometric techniques represent this type of mass movement (Figure 10). The geomorphometric map shows continuous, curved convex changes of slope bordered by concave changes of slope indicating the boundaries of a zone of elevated terrain (Figure 10a). These changes of slope delimit the snout and the flanks of the lobe and identify different textures on the lobe surfaces, such as the crests of pressure ridges. These have different patterns on the two lobes and can be easily discerned from the smoother surrounding areas (Figure 10a). The trough depth map (Figure 10b) shows how ridges characterize the accumulation zone of the lobes. These have a height of between 6.5 m and 13 m. The southern lobe (Figure 10b) is characterized by particularly high pressure ridges, as denoted by the blue arrow. Zones of low trough depths located outside the lobes, which demarcate the relatively smooth surrounding zones, are also important in distinguishing lobe boundaries. Slope gradient standard deviation (Figure 10c) marks the different surface textures of the lobes. The surface texture of the southern lobe is distinguished by a higher slope standard deviation compared to the northern lobe. This means that the surface of the southern lobe is rougher due to the presence of higher ridges (Figure 10c). The ISODATA thematic map shows the five classes of ridge morphologies (Figure 10d). The south-

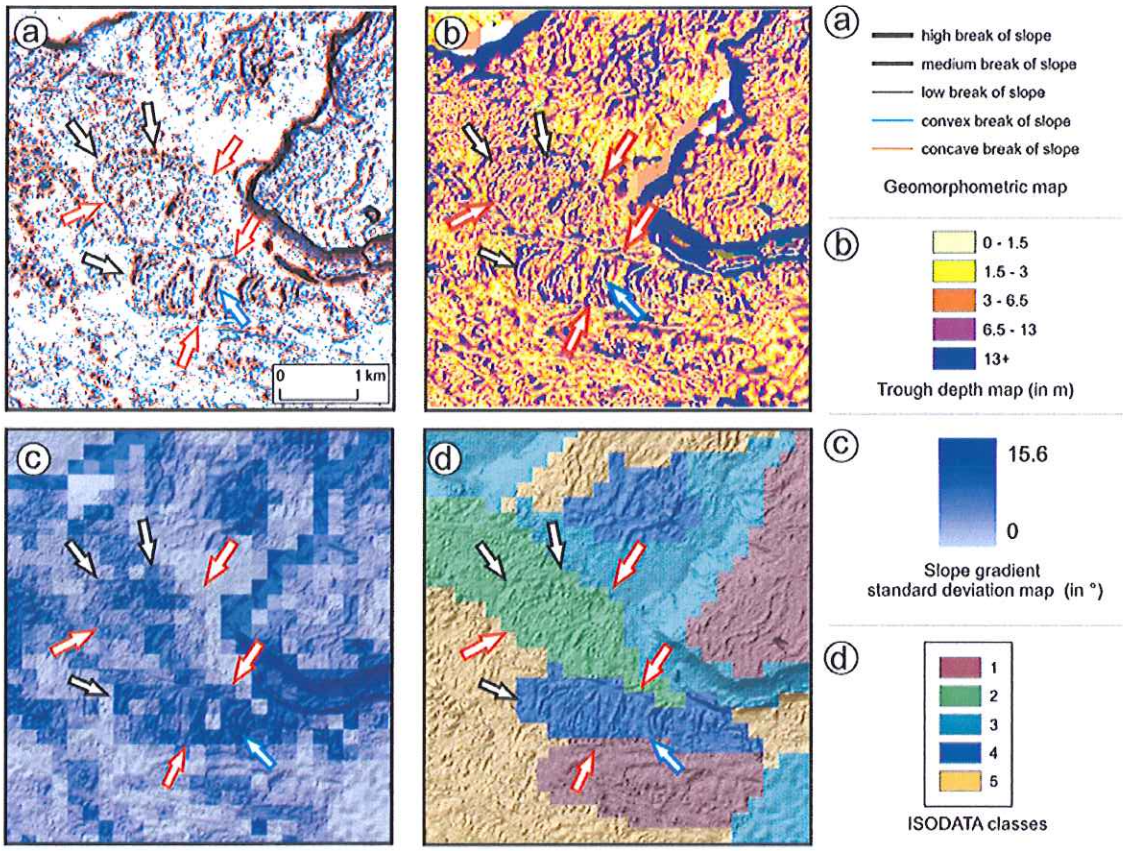

Figure 10. Results obtained when applying geomorphometric techniques on the area covering the two debris flow lobes: (a) geomorphometric map, (b) trough depth map, (c) slope gradient standard deviation map, and (d) ISODATA thematic map using ridge characteristics and slope gradient standard deviation as input layers. The black reference arrows denote the snout of the identified debris flow lobes, whereas the red and blue arrows indicate the flanks and pressure ridges, respectively.

ern debris flow lobe is represented by class 4, whereas the northern debris flow lobe is identified in class 2. The smoother surrounding topography is represented by class 3.

[45] The results demonstrate how geomorphometric techniques can be used to characterize the morphology of submarine debris flows. The resulting maps delimit the boundaries of morphological features and differentiate between different surfaces. When combined, they allow an accurate geomorphological interpretation of the site to be carried out. To demonstrate this, a comparison is made between two interpretative maps. The first map is redrawn from the interpretation of *Haflidason et al.* [2004] (Figure 11a). The second one (Figure 11c) is based on a morphological map produced combining the geomorphometric map with the ISODATA thematic map (Figure 11b). Using Figure 11b we were able to produce our interpretative map of the mass movements that have occurred within this area of Storegga. The two maps show the same interpretation in the northern part of the area. However, they vary in the representation of the debris flow lobes in the southern part of the area. The northern debris flow lobe, labeled "N1" in Figure 11c, has not been identified by *Haflidason et al.* [2004]. Furthermore, the boundaries of lobes E7 and E8 are interpreted as shorter and narrower, respectively (Figure 11c). Two new overlapping lobes, labeled "N2" and "N3," have been identified to the west and south of lobes E7 and E8.

5. Conclusions

[46] Geomorphometric techniques cannot be simply transferred from subaerial to submarine environments. A number of geomorphometric techniques have thus been adapted and developed for a submarine landscape. These techniques enable the extraction of high-order morphological features from DEM analysis, by allowing the delineation of morphological boundaries and the classification of surfaces into units with homogeneous topography. Morphometric attributes and their statistical analyses provide summary information about an area, which can be used to calibrate computer-generated geomorphometric maps. Geomorphometric mapping is best utilized to delineate the boundaries of morphological features and produce a base map for geomorphological interpretation. Ridge characterization identifies ridges and blocks in the topography and generates specific morphological information on terrain

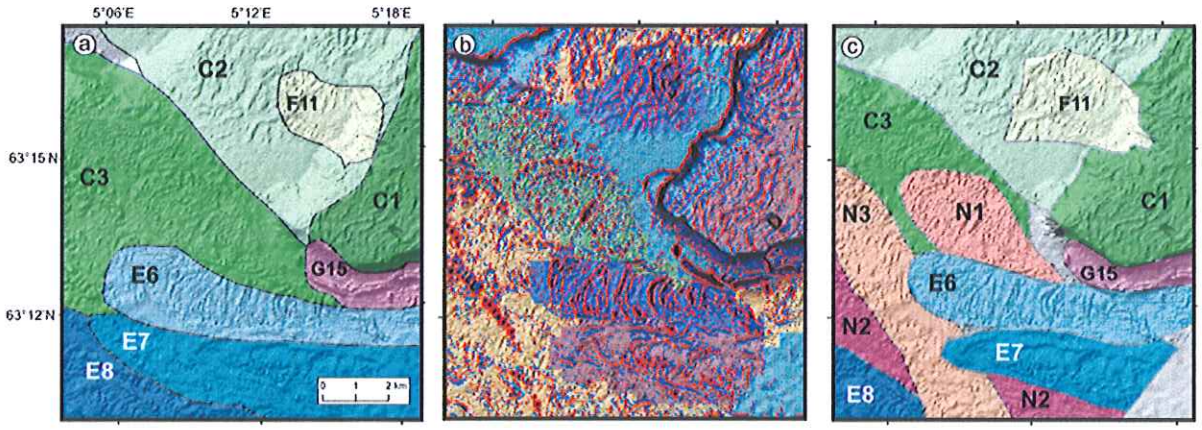

Figure 11. (a) Interpretative map of Figure 10 redrawn from Figure 12H of *Haflidason et al.* [2004], with permission from Elsevier. (b) Map combining the geomorphometric map in Figure 10a with the thematic map in Figure 10d. (c) An interpretative map of the same area produced from the interpretation of Figure 11b. The lowermost eastern corner of Figure 11c is noise.

variability. Moment statistics can be used as proxies for surface roughness, whereas ISODATA applied using ridge characteristics and moment statistics segments a terrain surface into classes according to variability in ridge morphology. By integrating these techniques it is possible to interpret the geomorphology of a submarine landscape more accurately, as shown by the comparison of the interpretation of debris flows as published by *Haflidason et al.* [2004] with an interpretative map drawn from the resulting maps of the proposed techniques.

[47] Geomorphometric approaches offer a number of benefits. The most important include (1) a greater spatial detail of analysis, (2) production of topographic information in quantitative format, (3) the generation of consistent and rapid results based on an established set of rules for landform delineation, and (4) the possibility to use the techniques and results with other digital data sources, such as side scan imagery or 3-D seismic data. Furthermore, the techniques are simple to use and morphological information can be read directly from one map. All of these improve the morphological interpretation of bathymetric maps. In comparison, manual methods of interpretation are more time consuming and subjective.

[48] A few caveats do apply to the use of geomorphometric techniques in submarine environments. Knowledge of the study area is required to evaluate the reliability of the results and to choose terrain attributes. The techniques are also heavily dependent upon scale and data resolution. As topographic complexity and patterns change as a function of scale, the comparison of results obtained from different resolutions is problematic. Nevertheless, geomorphometric methods of feature extraction and landscape classification are promising techniques for submarine data evaluation. For the best results they should augment, rather than replace, manual methods of interpretation. The increased availability and accuracy of bathymetry data sets in digital format offers a unique opportunity to improve these methodologies for the quantitative mapping of geomorphometric landforms.

[49] **Acknowledgments.** We would like to thank Norsk Hydro AS for providing the bathymetric data used in this study and Haflidi Haflidason, University of Bergen, for reviewing an earlier version of this paper.

References

Adediran, A. O., I. Parcharidis, M. Poscolieri, and K. Pavlopoulos (2004), Computer-assisted discrimination of morphological units on north-central Crete (Greece) by applying multivariate statistics to local relief gradients, *Geomorphology*, *58*, 357–370.

Aharonson, O., M. T. Zuber, and D. H. Rothman (2001), Statistics of Mars' topography from the Mars Orbiter Laser Altimeter: Slopes, correlation and physical models, *J. Geophys. Res.*, *106*(E10), 23,723–23,735.

Anhert, F. (1970), An approach towards a descriptive classification of slopes, *Z. Geomorphol. Suppl.*, *9*, 70–84.

Bryn, P., A. Solheim, K. Berg, R. Lein, C. F. Forsberg, H. Haflidason, D. Ottesen, and L. Rise (2003), The Storegga Slide Complex: Repeated large scale sliding in response to climatic cyclicity, in *Submarine Mass Movements and Their Consequences*, edited by J. Locat and J. Mienert, pp. 215–222, Springer, New York.

Bugge, T., S. Befring, R. H. Belderson, T. Eidvin, E. Jansen, N. H. Kenyon, H. Holtedahl, and H. P. Sejrup (1987), A giant three-stage submarine slide off Norway, *Geo Mar. Lett.*, *7*, 191–198.

Canals, M., et al. (2004), Slope failure dynamics and impacts from seafloor and shallow sub-seafloor geophysical data: Case studies from the COSTA project, *Mar. Geol.*, *213*(1–4), 9–72.

Carrara, A., E. Pugliese-Carratelli, and L. Merenda (1977), Computer based data banks and statistical analysis for slope instability phenomena, *Z. Geomorphol.*, *21*(2), 187–222.

Casas, A. M., A. L. Cortés, A. Maestro, M. A. Soriano, A. Riaguas, and J. Bernal (2000), LINDENS: A program for lineament length and density analysis, *Comput. Geosci.*, *26*, 1011–1022.

Chang, Y. C., G. S. Song, and S. K. Hsu (1998), Automatic extraction of ridge and valley axes using the profile recognition and polygon-breaking algorithm, *Comput. Geosci.*, *24*(1), 83–93.

Chorowicz, J., Y. J. Kim, S. Manoussis, J. P. Rudant, P. Foin, and Y. Veillet (1989), A new technique for recognition of geological and geomorphological patterns in digital terrain models, *Remote Sens. Environ.*, *29*, 229–239.

Chorowicz, J., C. Ichoko, S. Riazanoff, and Y. J. Kim (1992), A combined algorithm for automated drainage network extraction, *Water Resour. Res.*, *28*, 1293–1302.

Corominas, J., J. Remondo, P. Farias, M. Estevao, J. Zézere, D. T. Díaz, J. R. Dikau, L. Schrott, J. Moya, and A. Gonzáles (1996), Debris flows, in *Landslide Recognition: Identification, Movement and Causes*, edited by R. Dikau et al., pp. 161–180, John Wiley, Hoboken, N. J.

Curtis, L. F., J. C. Doornkamp, and K. J. Gregory (1965), The description of relief in field studies of soils, *J. Soil Sci.*, *16*, 16–30.

De Moustier, C., and H. Matsumoto (1993), Seafloor acoustic remote sensing with multibeam echo-sounders and bathymetric sidescan sonar system, *Mar. Geophys. Res.*, *15*, 27–42.

Duda, R. O., and P. E. Hart (1973), *Pattern Recognition and Scene Analysis*, John Wiley, Hoboken, N. J.

Etzelmüller, B., and J. R. Sulebak (2000), Development in the use of digital elevation models in periglacial geomorphology and glaciology, *Phys. Geogr.*, *41*, 35–58.

Evans, I. S. (1972), General geomorphometry, derivatives of altitude and descriptive statistics, in *Spatial Analysis in Geomorphology*, edited by R. J. Chorley, pp. 17–90, HarperCollins, New York.

Evans, I. S. (1975), The effect of resolution on gradients calculated from an altitude matrix, report 3 on statistical characterisation of altitude matrices by computer, 24 pp., Dep. of Geogr., Univ. of Durham, Durham, N. C.

Evans, I. S. (1979), An integrated system of terrain analysis and slope mapping, final report, Univ. of Durham, Durham, N. C.

Evans, I. S. (1980), An integrated system of terrain analysis and slope mapping, *Z. Geomorphol. Suppl.*, *36*, 274–295.

Evans, I. S. (1990), General geomorphometry, in *Geomorphological Techniques*, edited by A. S. Goudie et al., pp. 44–56, Routeledge, Boca Raton, Fla.

Evans, I. S. (1998), What do terrain statistics really mean?, in *Landform Monitoring, Modelling and Analysis*, edited by S. N. Lane, K. S. Richards, and J. H. Chandler, pp. 119–138, John Wiley, Hoboken, N. J.

Florinsky, I. (1996), Quantitative topographic method of fault morphology recognition, *Geomorphology*, *16*, 103–119.

Fox, C. G. (1996), Objective classification of oceanic ridge-crest terrains using two-dimensional spectral models of bathymetry: Application to the Juan de Fuca Ridge, *Mar. Geophys. Res.*, *18*(6), 707–728.

Gardiner, V., and R. Dackombe (1983), *Geomorphological Field Manual*, Allen and Unwin, St. Leonards, N. S. W., Australia.

Gardner, T. W., K. C. Sasowksy, and R. L. Day (1990), Automated extraction of geomorphometric properties from digital elevation data, *Z. Geomorphol. Suppl.*, *80*, 57–68.

Giles, P. T. (1998), Geomorphological signatures: Classification of aggregated slope unit objects from digital elevation and remote sensing data, *Earth Surf. Processes Landforms*, *23*, 581–594.

Graff, L. H., and E. L. Usery (1993), Automated classification of generic terrain features in digital elevation models, *Photogramm. Eng. Remote Sens.*, *59*(9), 1409–1417.

Guth, P. L. (2003), Eigenvector analysis of digital elevation models in a GIS: Geomorphometry and quality control, in *Concepts and Modelling in Geomorphology: International Perspectives*, edited by I. S. Evans et al., pp. 199–220, Terra Sci., Tokyo.

Haflidason, H., H. P. Sejrup, A. Nygård, P. Bryn, R. Lien, C. F. Forsberg, K. Berg, and D. G. Masson (2004), The Storegga Slide: Architecture, geometry and slide-development, *Mar. Geol.*, *231*, 201–234.

Haflidason, H., R. Lien, H. P. Sejrup, C. F. Forsberg, and P. Bryn (2005), The dating and morphometry of the Storegga Slide, *Mar. Pet. Geol.*, *22*(1–2), 123–136.

Hall, D. J., and D. Khanna (1977), *Statistical Methods for Digital Computers*, John Wiley, Hoboken, N. J.

Hühnerbach, V., and D. G. Masson (2004), Landslides in the North Atlantic and its adjacent seas: An analysis of their morphology, setting and behaviour, *Mar. Geol.*, *213*, 343–362.

Irvin, B. J., S. J. Ventura, and B. K. Slater (1997), Fuzzy and isodata classification of landform elements from digital terrain data in Pleasant Valley, Wisconsin, *Geoderma*, *77*, 137–154.

Johnson, A. M. (1984), Debris flows, in *Slope Instability*, edited by D. Brunsden, and D. B. Prior, pp. 257–362, John Wiley, Hoboken, N. J.

Masson, D. G., C. B. Harbitz, R. B. Wynn, G. Pedersen, and F. Løvholt (2006), Submarine landslides: Processes, triggers and hazard prediction, *Philos. Trans. R. Soc., Ser. A*, *364*(1845), 2009–2039.

Medler, M. J., and S. R. Yool (1998), Computer-assisted terrain stratification, *Phys. Geogr.*, *19*(5), 433–443.

Moore, I. D., and J. L. Neiber (1989), Landscape assessment of soil erosion and non-point source pollution, *J. Minn. Acad. Sci.*, *55*, 18–24.

Moore, I. D., R. B. Grayson, and A. R. Ladson (1991), Digital terrain modelling: A review of hydrological, geomorphological and biological applications, *Hydrol. Processes*, *5*(1), 3–30.

Mulder, R., and P. Cochonat (1996), Classification of offshore mass movements, *J. Sediment. Res.*, *66*(1), 43–57.

Nogami, M. (1995), Geomorphometric measures for digital elevation models, *Z. Geomorphol. Suppl.*, *101*, 53–67.

Nygård, A., H. P. Sejrup, H. Haflidason, and E. L. King (2002), Geometry and genesis of glacigenic debris flows on the North Sea Fan: TOBI imagery and deep-tow boomer evidence, *Mar. Geol.*, *188*, 15–33.

Parsons, A. J. (1988), *Hillslope Form*, Routledge, Boca Raton, Fla.

Pike, R. J. (2000), Geomorphometry—Diversity in quantitative surface analysis, *Prog. Phys. Geogr.*, *21*(1), 1–20.

Pike, R. J., and R. Dikau (1995), Advances in geomorphometry, *Z. Geomorphol., Suppl.*, *101*, 1–238.

Pratson, L. F., and W. B. F. Ryan (1996), Automated drainage extraction in mapping the Monterey submarine drainage system, California margin, *Mar. Geophys. Res.*, *18*(6), 757–777.

Prior, D. B., J. M. Coleman, and B. D. Bornhold (1982), Results of a known seafloor instability event, *Geo Mar. Lett.*, *2*, 117–122.

Raghavan, V., S. Masumoto, K. Koike, and S. Nagano (1995), Automatic lineament extraction from digital images using a segment tracing and rotation transformation approach, *Comput. Geosci.*, *21*(4), 555–591.

Richards, J. A. (1986), *Remote Sensing Digital Image Analysis: An Introduction*, Springer, New York.

Roering, J. J., J. W. Kirchner, and W. E. Dietrich (2005), Characterizing structural and lithological controls on deep-seated landsliding: Implications for topographic relief and landscape evolution in the Oregon Coast Range, USA, *Geol. Soc. Am. Bull.*, *117*, 654–668.

Shepard, F. P. (1963), *Submarine Geology*, 2nd ed., HarperCollins, New York.

Sulebak, J. R., B. Etzelmüller, and J. L. Sollid (1997), Landscape regionalization by automatic classification of landform elements, *Nor. Geogr. Tidsskr.*, *51*, 35–45.

C. Berndt, D. G. Masson, A. Micallef, and D. A. V. Stow, National Oceanography Centre, Southampton, European Way, Southampton, SO14 3ZH, UK. (amicall@noc.soton.ac.uk)